J. Chem. Eng. Data 1991, 36, 236-240

Measurements of *PVTx* Properties for the Binary Refrigerant HCFC 142b + HCFC 22 System

Katsuhiko Kumagai, Naoyuki Yada,* Haruki Sato, and Koichi Watanabe

Department of Mechanical Engineering, Faculty of Science and Technology, Keio University, 3-14-1, Hiyoshi, Kohoku-ku, Yokohama 223, Japan

This paper reports *PVTx* properties for the HCFC 142b + HCFC 22 system in a wide range of temperatures from 297 to 443 K, of pressures from 0.5 to 10.0 MPa, and of densities from 72 to 1079 kg/m^3. For 4 compositions, i.e., 20, 40, 60, and 80 wt % HCFC 142b, 422 *PVTx* measurements have been made along 31 isochores. The uncertainties of the temperature, pressure, and density measurements are less than ±10 mK, ±3.0 kPa, and ±0.1%, respectively. From the *PVTx* measurements for 20, 40, 60, and 80 wt % HCFC 142b, we have determined dew points and bubble points, enabling us to construct the dew- and bubble-point curves for each composition. We have also compared the vapor–liquid equilibrium data along three isotherms, where the experimental data are reported by others, with the vapor–liquid equilibrium curve calculated from the Raoult's law.

Introduction

The advantage of using binary refrigerant mixtures for refrigeration and heat pump systems as well as Rankine cycle applications with small temperature difference has been pointed out and discussed in many references (*1*). The *PVTx* properties of binary refrigerant mixtures should be known accurately not only for the system design but also for reliable assessment of the cycle performance.

Although the binary refrigerant mixture of the hydrochlorofluorocarbon (HCFC) 142b (CH_3CClF_2, 1-chloro-1,1-difluoroethane) and HCFC 22 ($CHClF_2$, chlorodifluoromethane) system is one of the technically important mixtures, experimental measurements of the thermodynamic properties of this system have not been available up to now. The HCFC 142b + HCFC 22 system has been proposed as a promising candidate to replace CFC 12 (*2*), because of the low ozone depletion potentials of HCFC 142b and HCFC 22.

In our previous publications, we have reported the *PVTx* measurements for the CFC 12 + HCFC 22 system (*3*), the HCFC 22 + CFC 114 system (*4*), the Halon 1301 + CFC 114 system (*5*), the HFC 152a + CFC 114 system (6), and the CFC 115 + CFC 114 system (*7*, *8*), respectively. In this paper we report the thermodynamic properties of the HCFC 142b + HCFC 22 system in a wide range of temperatures from 297 to 443 K, of pressures from 0.5 to 10.0 MPa, and of densities from 72 to 1079 kg/m^3. We have measured 442 *PVTx* properties for 4 compositions, i.e., 20, 40, 60, and 80 wt % HCFC 142b along 31 isochores. On the basis of the experimental data, we have determined dew points and bubble points for representing the dew- and bubble-point curves of each mixture with different composition.

Experimental Section

The method, apparatus, and procedure of the *PVTx* measurements used here have been described in detail in our previous publications (*9*, *10*). In principle, the *PVTx* measurements of this work were made by a constant-volume method coupled with isothermal expansion procedures. Figure 1 shows a schematic diagram of the apparatus used.

Prescribed quantities of 99.98, 99.82, and/or 99.9 wt % pure HCFC 142b, and that of 99.97 wt % pure HCFC 22, were prepared in two independent vessels, which had been evacuated in advance. The amount of the pure component in each vessel was adjusted by weighing to the necessary mass by means of a precision chemical balance with a sensitivity of 2 mg. The temperature was measured by a 25-Ω platinum resistance thermometer calibrated on the IPTS-68 within ±5 mK. The temperature in the thermostated bath is controlled within ±5 mK. Thus the uncertainty of the temperature measurements was less than ±10 mK. Since the sample temperature was not measured directly in the present measurements, careful attention has been given to verify the existence of thermodynamic equilibrium between the sample and the thermostated bath fluid during the experiments. The sample pressure was transmitted to an external pressure measuring system through a diaphragm-type differential pressure detector by balancing the sample pressure with the pressure of the nitrogen gas applied as the pressure transmitting medium. The sensitivity of the pressure measurements was about 0.1 kPa. The nitrogen pressure was measured with two different pressure gauges: an air piston gauge for pressures below 4.2 MPa and an oil-operated dead weight pressure gauge for pressures above 4.2 MPa. The uncertainty of the pressure measurements was less than ±1.4 kPa for pressures below 4.2 MPa, whereas less than ±3.0 kPa for those above 4.2 MPa. The uncertainty of the density measurements after the expansion procedure accumulates by repeating the expansions. Since the expansion procedures did not exceed three times in the present study, the uncertainty of the density measurements was estimated to be less than ±0.1%. The uncertainty of the mass fraction measurements was also estimated to be less than ±0.1%.

Results

The experiments have been carried out for four compositions, namely, 20, 40, 60, and 80 wt % HCFC 142b. Table I summarizes all of the experimental data, including the vapor–liquid coexistence data in the two-phase region (those data are identified by footnote a in Table I). The distribution of the measured points is shown in Figure 2. Nine Series of the *PVTx* measurements for the mixture of 20 wt % (17.7 mol %) HCFC 142b + 80 wt % (82.3 mol %) HCFC 22 cover the density range from 80 to 985 kg/m^3. Table I gives 135 *PVTx* data for this composition, including 54 data in the two-phase region. For the mixture of 40 wt % (36.5 mol %) HCFC 142b + 60 wt % (63.5 mol %) HCFC 22, the observations correspond to the densities from 85 to 1079 kg/m^3. Table I lists 81 *PVTx* data for this composition along 6 isochores, including 30 measurements in the two-phase region. For the mixture of 60 wt % (56.3 mol %) HCFC 142b + 40 wt % (43.7 mol %) HCFC 22, the measurements cover the densities from 95 to 1047 kg/m^3. The 96 *PVTx* data along 7 isochores, including 44 data in the vapor–liquid coexisting region, are tabulated in Table I. Nine

* To whom correspondence should be addressed.

0021-9568/91/1736-0236$02.50/0

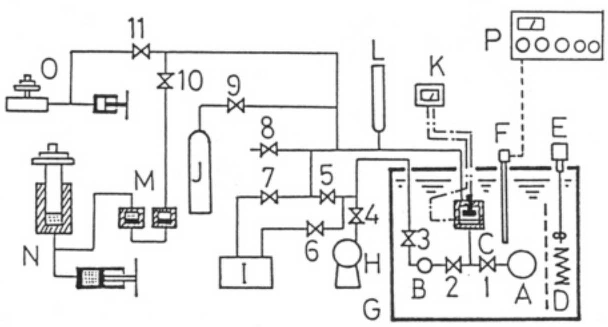

A: Sample cell; B: Expansion cell; C: Differential pressure detector; D: Heater; E: Stirrer; F: Platinum resistance thermometer; G: Thermostated bath; H: Vacuum pump; I: Bourdon tube differential pressure gage; J: Nitrogen cylinder; K: Electronic device for detecting differential pressure; L: Nitrogen gas damper; M: Oil-gas separator; N: Oil-operated dead weight pressure gage; O: Air-piston gage; P: Temperature bridge; 1–11: Valves

Figure 1. Schematic diagram of the apparatus.

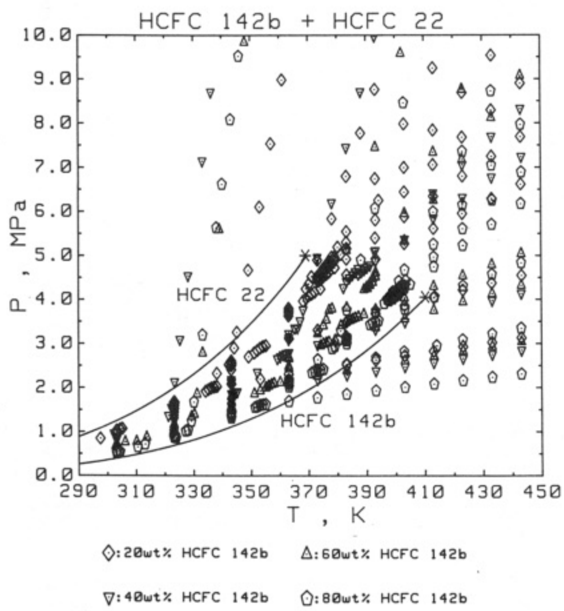

Figure 2. Distribution of the measurements for the HCFC 142b + HCFC 22 system in a pressure–temperature diagram.

series of the *PVTx* measurements for the mixture of 80 wt % (77.5 mol %) HCFC 142b + 20 wt % (22.5 mol %) HCFC 22 cover the density range from 72 to 1038 kg/m^3. Table I gives 130 *PVTx* data for this composition, including 63 data in the two-phase region.

Analyzing these *PVTx* measurements graphically for four compositions, we determined the dew and bubble points by finding the breaking point of each isochore on the *P–T* plane. We determined the bubble point as the breaking point where the slope of the isochore increases, while the dew point was determined as the breaking point where the slope of the isochore decreases. Table II summarizes the dew points and bubble points for each composition of the HCFC 142b + HCFC 22 system with their uncertainties. When the isochore is nearer to the critical density, it is not so easy to identify the breaking point accurately because the measured data in the critical region is accompanied by some larger uncertainties. In spite of the importance of determining the critical points of the mixtures precisely, it seems to us rather premature to provide the critical point data, only from the present measurements. We are expecting, however, that a set of the critical parameter values for the present binary mixtures will be provided through the direct observation of the meniscus disappearance currently being

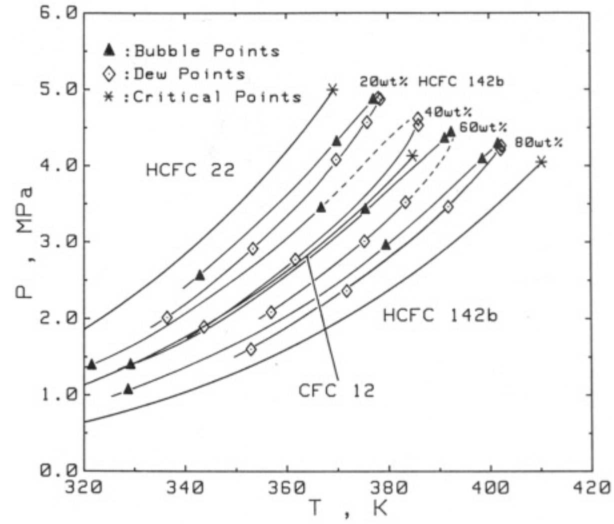

Figure 3. Dew and bubble points of the HCFC 142b + HCFC 22 system.

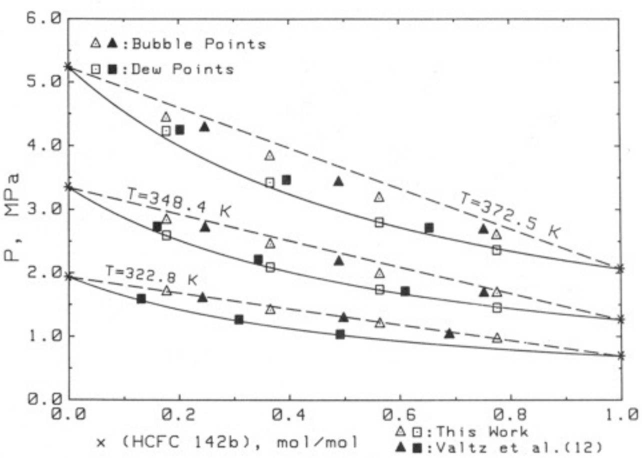

Figure 4. Comparison of the vapor–liquid coexistence data for the HCFC 142b + HCFC 22 system.

undertaken by our group at the Thermodynamics Laboratory, Keio University, Yokohama, Japan (*11*).

Discussion

The dew points and bubble points listed in Table II are shown on the *P–T* plane in Figure 3, together with the vapor pressure curves and critical points of pure components HCFC 142b and HCFC 22. In addition, those of CFC 12 are also drawn for comparison with dew- and bubble-point curves of the 60 wt % HCFC 142b mixture. Connecting the dew and bubble points smoothly, we can obtain dew- and bubble-point curves from which dew points and bubble points at arbitrary temperatures or pressures can be deduced.

We find that the dew- and bubble-point curves of the HCFC 142b + HCFC 22 system are distributed almost evenly with their difference in weight fractions. From the envelope of the dew- and bubble-point curves in Figure 3, it is seen that this mixture is a nonazeotropic one that has different dew-point and bubble-point curves. Among the four compositions, the composition that has the largest envelope of dew- and bubble-point curve is 60 wt % HCFC 142b. The spread of the phase-boundary envelope for 20 wt % HCFC 142b is as large as that of 80 wt % HCFC 142b. Comparing the vapor pressure curve of CFC 12 with dew- and bubble-point curves of this mixture in Figure 3, we found that this mixture was reconfirmed as a substitute for CFC 12, as proposed in ref 2. The dew-point curve of 40 wt % HCFC 142b and the bubble-point curve of

Table I. Experimental Data[a]

ρ, kg/m^3	T, K	P, MPa	ρ, kg/m^3	T, K	P, MPa	ρ, kg/m^3	T, K	P, MPa
			20 wt % (17.7 mol %) HCFC 142b + 80 wt % HCFC 22					
984.9*	303.183	1.0259	469.9	433.244	9.5323	235.8	413.157	5.6129
984.0*	323.126	1.6754	471.4*	373.120	4.4713	235.7	423.062	5.9510
983.3*	338.110	2.3232	471.3*	375.013	4.6265	235.6	433.185	6.2896
982.9	345.114	3.2536	471.3*	377.152	4.8011	235.5	443.184	6.6188
982.6	349.130	4.6671	471.2	379.116	4.9648	236.4*	368.127	3.9599
982.4	353.112	6.0979	470.9	394.322	6.2489	236.3	370.109	4.0801
982.1	357.092	7.5302	375.4*	323.157	1.6573	236.3	372.149	4.1620
981.9	361.094	8.9779	375.0*	343.172	2.5430	236.3	374.151	4.2380
983.1*	342.178	2.5197	374.7*	363.132	3.7224	236.3	371.125	4.1205
983.0	343.094	2.6029	374.5*	373.150	4.4326	140.2*	303.057	0.9976
982.9	344.118	2.8994	374.3	383.162	5.1599	140.1*	323.136	1.6031
782.4*	303.152	1.0270	373.9	403.159	6.4371	139.9*	343.105	2.4085
781.7*	323.216	1.6767	373.7	413.096	7.0598	139.8	363.180	3.1104
780.9*	343.134	2.5755	373.5	423.163	7.6774	139.7	383.174	3.4924
780.1*	363.132	3.7987	373.3	433.160	8.2909	139.5	403.126	3.8584
779.7	373.139	4.8963	373.1	443.192	8.8981	139.5	413.181	4.0376
779.3	383.141	6.7932	374.4*	375.125	4.5852	139.4	423.175	4.2131
778.8	393.173	8.7591	374.4*	377.162	4.7416	139.3	433.078	4.3746
779.9*	369.097	4.2371	374.4*	378.126	4.8161	139.2	443.286	4.5463
779.9	370.158	4.3523	374.3	379.127	4.8904	139.9*	349.145	2.6954
779.8	371.119	4.5215	374.3	381.132	5.0248	139.9*	351.109	2.7884
779.5	378.137	5.8313	374.1	393.155	5.8067	139.9*	352.122	2.8385
779.1	388.138	7.7709	298.5*	303.218	1.0213	139.9*	353.110	2.8906
621.5*	304.325	1.0545	298.2*	323.135	1.6531	139.9	354.099	2.9271
621.0*	323.147	1.6734	297.9*	343.166	2.5284	139.9	355.121	2.9480
620.4*	343.116	2.5717	297.6*	363.137	3.6887	139.7	373.171	3.3034
619.8*	363.159	3.7870	297.3	383.143	4.9206	139.6	393.079	3.6767
619.1	383.147	5.5411	297.0	403.160	5.8769	88.5*	297.487	0.8433
618.8	393.131	6.7425	296.9	413.158	6.3409	88.4*	323.157	1.5327
618.4	403.117	7.9767	296.7	423.205	6.7981	88.3	343.141	2.0822
618.1	413.188	9.2492	296.6	433.193	7.2483	88.3	353.199	2.1940
619.4*	373.148	4.5274	296.4	443.166	7.6899	88.2	373.155	2.4112
619.4*	375.116	4.6966	297.5*	373.661	4.4167	88.3*	334.141	1.9168
619.3*	376.142	4.7787	297.4*	375.111	4.5074	88.3*	335.162	1.9524
619.3*	377.088	4.8660	297.4	376.156	4.5685	88.3*	336.152	1.9876
619.3	378.095	4.9656	297.4	377.088	4.6165	88.3	337.166	2.0081
619.2	380.136	5.1895	297.4	379.126	4.7219	88.3	338.141	2.0234
473.0*	303.134	1.0183	297.2	393.062	5.3989	88.2	363.094	2.3035
472.5*	323.133	1.6586	237.1*	305.132	1.0687	88.1	383.121	2.5171
472.1*	343.131	2.5498	236.9*	323.132	1.6435	88.1	393.143	2.6210
471.6*	363.110	3.7438	236.7*	343.103	2.5008	88.0	403.084	2.7227
471.1	383.121	5.2986	236.4*	363.089	3.6253	88.0	413.066	2.8243
470.6	403.147	6.9930	236.2	383.156	4.5615	88.0	423.172	2.9262
470.4	413.165	7.8372	236.1	393.185	4.9210	87.9	433.099	3.0246
470.1	423.161	8.6849	235.9	403.113	5.2686	87.9	443.181	3.1245
			40 wt % (36.5 mol %) HCFC 142b + 60 wt % HCFC 22					
1079.4*	303.216	0.8670	396.0*	384.128	4.4934	134.9*	323.126	1.3191
1078.3	323.333	2.1350	396.0*	385.139	4.5636	134.8*	343.133	2.1016
1078.2	325.227	3.0945	396.0*	386.127	4.6321	134.6	363.139	2.7962
1078.5*	321.168	1.3649	396.0	387.130	4.7066	134.6	373.133	2.9771
1078.4	322.168	1.5520	395.8	392.865	5.0964	134.5	383.138	3.1523
1078.0	328.105	4.5418	395.8	393.163	5.1177	134.7*	352.137	2.3501
1077.6	333.260	7.1461	395.4	413.111	6.4185	134.7*	359.132	2.6574
1077.3	336.325	8.7028	395.2	423.150	7.0616	134.7*	360.142	2.7022
857.6*	302.181	0.9595	395.0	433.171	7.6955	134.6*	361.165	2.7483
856.7*	323.132	1.4171	394.8	443.160	8.3253	134.6	362.160	2.7778
855.9*	343.082	2.1838	315.9*	303.157	0.8483	134.4	393.073	3.3219
855.1*	363.097	3.2249	315.6*	323.249	1.3880	134.4	403.212	3.4925
854.6	373.124	4.9633	315.3*	343.159	2.1232	134.2	433.174	3.9778
854.1	383.160	7.4506	315.0*	363.094	3.0943	134.1	443.161	4.1364
853.8	388.155	8.7102	314.7*	382.092	4.2726	85.1*	323.135	1.2583
855.0*	365.156	3.3488	314.5	393.148	4.8788	85.1*	343.143	1.8643
854.9*	366.160	3.3519	314.3	403.183	5.3732	85.0	363.143	2.0905
854.9	367.057	3.5171	314.2	413.163	5.8494	84.9	373.156	2.1895
854.8	368.153	3.7650	314.0	423.192	6.3164	84.9	383.187	2.2890
854.8	369.179	4.0086	313.8	433.179	6.7739	85.1	344.143	1.8952
854.3	378.135	6.1978	313.7	443.391	7.2423	85.2	345.141	1.9045
853.6	393.092	9.9739	314.6	387.184	4.5780	84.9	393.171	2.3834
397.6*	303.131	0.8501	314.6	388.178	4.6307	84.8	403.198	2.4786
397.2*	323.135	1.3932	314.5	389.191	4.6814	84.8	413.114	2.5721
396.8*	343.138	2.1427	314.5	390.168	4.7332	84.7	423.148	2.6650
396.4*	363.147	3.1357	314.5	391.182	4.7832	84.7	433.167	2.7557
396.0*	383.147	4.4151	135.0*	303.139	0.8229	84.6	443.205	2.8478

Table I (Continued)

ρ, kg/m^3	T, K	P, MPa	ρ, kg/m^3	T, K	P, MPa	ρ, kg/m^3	T, K	P, MPa
			60 wt % (56.3 mol %) HCFC 142b + 40 wt % HCFC 22					
1047.1*	306.108	0.7640	660.0	393.158	4.6121	150.6*	323.020	1.0886
1046.3*	323.113	1.1681	526.7*	303.140	0.7039	150.4*	343.203	1.6715
1045.3	339.116	5.5901	526.2*	323.122	1.1591	150.3*	363.162	2.4347
1044.7	348.137	9.8392	525.7*	343.149	1.7982	150.1	383.010	3.1551
1046.0*	329.139	1.3423	525.2*	363.149	2.6598	150.0	403.182	3.5603
1046.0	330.157	1.3950	524.8*	378.142	3.7896	149.9	413.157	3.7537
1045.9	331.143	1.8553	524.1	403.207	5.3336	149.8	423.183	3.9447
1045.8	333.124	2.7868	523.8	413.216	6.2506	149.8	433.176	4.1318
832.0*	303.239	0.7087	523.6	423.049	7.1751	149.7	443.173	4.3183
831.3*	323.142	1.1676	523.3	433.182	8.1204	150.2*	374.147	2.9503
830.5*	343.130	1.8130	523.0	443.170	9.0700	150.2*	375.154	2.9918
829.7*	363.142	2.6867	524.5*	390.139	4.2469	150.2	376.185	3.0126
829.2*	373.147	3.2268	524.4*	391.146	4.3189	150.2	377.114	3.0327
828.8	383.154	5.1192	524.4*	392.145	4.3923	150.2	379.181	3.0756
828.3	393.161	7.4505	189.7*	302.723	0.6756	150.1	393.139	3.3635
827.8	402.151	9.5776	189.5*	323.098	1.1126	95.1*	310.096	0.7758
829.2*	373.097	3.2227	189.4*	343.083	1.7065	95.0*	323.145	1.0491
829.2*	375.132	3.4021	189.2*	363.081	2.4857	94.9*	343.108	1.5907
829.1	376.144	3.5354	189.0*	383.084	3.4874	94.8	373.021	2.2712
829.1	377.134	3.7570	188.8	403.084	4.0346	94.7	383.142	2.3874
662.9*	303.142	0.7072	188.6	423.164	4.5400	94.6	403.172	2.6094
662.3*	323.142	1.1631	188.5	433.154	4.7924	94.9*	351.125	1.8589
661.7*	343.150	1.8029	188.4	443.191	5.0407	94.9*	353.158	1.9293
661.1*	363.163	2.6720	189.0*	381.153	3.4030	94.9*	355.113	1.9969
660.4*	383.164	3.8128	189.0	384.122	3.5203	94.9*	356.124	2.0374
659.7	403.159	5.9524	189.0	385.149	3.5478	94.9	357.138	2.0733
659.3	413.160	7.3399	189.0	386.106	3.5776	94.8	358.033	2.0936
658.9	423.099	8.7596	189.0	387.222	3.6057	94.8	360.128	2.1194
660.2*	389.135	4.2203	188.9	389.095	3.6573	94.6	413.167	2.7189
660.2*	390.174	4.2827	188.9	393.119	3.7691	94.5	423.178	2.8265
660.1	391.151	4.3574	188.7	413.142	4.2982	94.5	433.167	2.9334
660.1	392.162	4.4802	150.6*	313.600	0.8741	94.5	443.174	3.0378
			80 wt % (77.5 mol %) HCFC 142b + 20 wt % HCFC 22					
1038.1*	310.524	0.6488	518.1	403.565	4.4256	198.5*	383.151	2.9905
1037.5*	323.131	0.9171	517.8	413.181	5.2527	198.3	403.176	3.7773
1036.6	338.135	5.6271	517.2	433.176	7.0467	198.2	413.460	4.0600
1036.4	340.156	6.6161	517.0	443.206	7.9659	198.1	423.246	4.3083
1036.2	343.150	8.0753	517.5	423.141	6.1371	198.0	433.175	4.5712
1036.0	346.096	9.5173	518.2*	398.154	4.0441	197.9	443.217	4.8328
1037.3*	327.145	1.0113	518.2*	399.141	4.1100	198.4*	391.188	3.4233
1037.3*	328.040	1.0353	518.2*	400.081	4.1750	198.4	392.077	3.4585
1037.2	329.157	1.2370	518.1*	401.168	4.2528	198.4	393.147	3.4905
1037.1	330.046	1.6733	518.1	402.149	4.3129	198.4	394.136	3.5199
1036.9	333.150	3.1929	397.5*	304.082	0.5519	114.9*	304.399	0.5389
825.0*	303.278	0.5449	397.2*	232.581	0.9137	114.8*	323.111	0.8669
824.2*	323.123	0.9172	396.8*	343.142	1.4281	114.7*	343.122	1.3542
823.4*	343.106	1.4473	396.4*	363.210	2.1411	114.6*	363.183	2.0144
822.6*	363.177	2.1791	396.0*	383.125	3.0834	114.5	383.145	2.5311
821.8	383.161	3.7606	395.6	403.193	4.3144	114.4	402.926	2.8104
820.8	403.038	8.4549	395.4	413.193	4.9656	114.3	414.140	2.9490
822.2*	373.152	2.6305	395.0	433.364	6.2528	114.2	423.069	3.0816
822.0*	378.137	2.8829	394.8	443.395	6.8882	114.2	433.191	3.2143
822.0*	379.060	2.9313	395.7*	397.789	3.9643	114.1	443.109	3.3438
821.9	380.229	3.0791	395.7*	399.120	4.0513	114.5*	371.153	2.3373
821.9	381.117	3.2826	395.7*	400.176	4.1223	114.5	372.104	2.3666
821.5	388.126	4.8960	395.6*	401.154	4.1859	114.5	373.092	2.3818
821.3	393.105	6.0665	365.6*	402.160	4.2575	114.5	374.140	2.3976
655.4*	303.143	0.5438	395.2	423.202	5.6062	114.5	375.126	2.4121
654.8*	323.234	0.9179	315.8*	303.032	0.5349	114.4	393.114	2.6717
654.1*	343.175	1.4485	315.5*	323.486	0.9096	72.5*	303.140	0.5089
653.5*	363.121	2.1736	315.2*	343.259	1.4232	72.4*	323.846	0.8540
652.8*	383.152	3.1421	314.9*	363.153	2.1230	72.4*	343.150	1.3099
652.2	403.190	4.6738	314.6*	383.122	3.0579	72.3	363.160	1.6891
651.4	423.216	7.3554	314.3	403.191	4.2556	72.3	373.030	1.7703
651.1	433.151	8.7238	313.9	423.212	5.2266	72.2	383.101	1.8513
652.5*	393.149	3.7332	313.8	433.192	5.7023	72.3*	351.359	1.5512
652.4*	396.116	3.9081	313.6	443.197	6.1723	72.3*	352.112	1.5732
652.4*	397.117	3.9990	314.3*	399.084	4.0084	72.3	353.112	1.6010
652.3*	398.195	4.0774	314.3*	400.146	4.0726	72.3	354.092	1.6116
652.3	399.135	4.1716	314.3*	401.119	4.1363	72.3	355.081	1.6198
652.2	401.165	4.4118	314.3*	402.165	4.1986	72.2	393.155	1.9312
651.8	413.143	5.9844	314.2	405.111	4.3440	72.2	403.160	2.0071
520.4*	313.089	0.7116	314.1	413.237	4.7450	72.1	413.168	2.0847
520.1*	323.194	0.9118	199.1*	323.321	0.8942	72.1	423.144	2.1604
519.6*	343.167	1.4442	198.9*	343.133	1.3961	72.0	433.166	2.2345
519.1*	363.130	2.1670	198.7*	363.147	2.0820	72.0	443.139	2.3076
518.6*	383.155	3.1289						

[a] Values with an asterisk were measured at a state of vapor–liquid coexistence. The values of density and mass fraction in this state are only nominal.

Table II. Determined Dew and Bubble Points

	ρ, kg/m³	T, K	P, MPa
20 wt % (17.7 mol %) HCFC 142b			
dew point	88.3 ± 0.1	336.4 ± 0.7	2.01 ± 0.05
dew point	139.9 ± 0.1	353.3 ± 0.9	2.91 ± 0.06
dew point	236.4 ± 0.1	369.8 ± 1.3	4.08 ± 0.07
dew point	297.4 ± 0.1	375.9 ± 1.4	4.57 ± 0.08
dew point	374.4 ± 0.1	378.5 ± 2.0	4.87 ± 0.10
dew point	471.3 ± 0.1	378.1 ± 2.5	4.89 ± 0.15
bubble point	619.3 ± 0.1	377.1 ± 1.2	4.86 ± 0.09
bubble point	779.9 ± 0.1	369.9 ± 0.7	4.31 ± 0.07
bubble point	983.1 ± 0.1	342.9 ± 0.6	2.55 ± 0.06
40 wt % (36.5 mol %) HCFC 142b			
dew point	85.1 ± 0.1	343.7 ± 0.5	1.89 ± 0.04
dew point	134.6 ± 0.1	361.7 ± 0.6	2.77 ± 0.05
dew point	314.6 ± 0.1	386.0 ± 1.6	4.53 ± 0.09
dew point	396.0 ± 0.1	385.9 ± 1.8	4.62 ± 0.10
bubble point	855.0 ± 0.1	366.8 ± 0.7	3.44 ± 0.06
bubble point	1078.5 ± 0.1	321.5 ± 0.4	1.38 ± 0.05
60 wt % (56.3 mol %) HCFC 142b			
dew point	94.9 ± 0.1	356.9 ± 0.6	2.08 ± 0.05
dew point	150.2 ± 0.1	375.3 ± 0.7	3.01 ± 0.05
dew point	189.0 ± 0.1	383.4 ± 0.9	3.52 ± 0.07
bubble point	524.4 ± 0.1	392.4 ± 2.1	4.43 ± 0.14
bubble point	660.1 ± 0.1	391.1 ± 1.0	4.35 ± 0.08
bubble point	829.1 ± 0.1	375.5 ± 0.7	3.42 ± 0.07
bubble point	1046.0 ± 0.1	329.2 ± 0.5	1.39 ± 0.06
80 wt % (77.5 mol %) HCFC 142b			
dew point	72.3 ± 0.1	352.9 ± 0.6	1.60 ± 0.05
dew point	114.5 ± 0.1	371.8 ± 0.8	2.36 ± 0.05
dew point	198.4 ± 0.1	391.8 ± 0.9	3.46 ± 0.06
dew point	314.3 ± 0.1	402.3 ± 1.2	4.21 ± 0.08
dew point	395.6 ± 0.1	402.4 ± 2.0	4.26 ± 0.09
bubble point	518.1 ± 0.1	401.7 ± 1.4	4.28 ± 0.10
bubble point	652.3 ± 0.1	398.6 ± 0.8	4.08 ± 0.07
bubble point	822.0 ± 0.1	379.5 ± 0.5	2.95 ± 0.06
bubble point	1037.3 ± 0.1	328.7 ± 0.4	1.06 ± 0.04

60 wt % HCFC 142b locate at the position near the vapor pressure curve of CFC 12, as shown in Figure 3.

For the HCFC 142b + HCFC 22 system, Valtz et al. (*12*) reported the saturated liquid densities and bubble-point pressures along four isotherms, and then they calculated the saturated vapor densities and dew-point pressures with the aid of the Peng–Robinson equation. We prepared Figure 4 to compare our dew- and bubble-point data with values reported by Valtz et al. along three isotherms, i.e., 322.8, 348.4, and 372.5 K. In Figure 4 solid symbols indicate values reported by Valtz et al., including their calculated values, while other symbols indicate those by the present study. It should be noted, however, that our dew and bubble points have been interpolated so as to compare them along the common isotherms reported by Valtz et al., in Figure 4. The broken curves and solid curves in Figure 4 indicate the bubble-point and dew-point curves calculated from the Raoult's law, respectively.

Although the bubble-point pressure data at 372.5 and 348.4 K by Valtz et al. (*12*) are in good agreement with our data, both data show lower pressure than the Raoult's law. On the other hand, both sets of the dew- and bubble-point data agree well with the Raoult's law at 322.8 K. Our dew-point pressure data show a good agreement with Raoult's law at 372.5 and 348.4 K.

Acknowledgment

We are greatly indebted to the National Research Laboratory of Metrology, Tsukuba, Japan, for calibration of the thermometer, to Shin-etsu Chemicals Co., Ltd., Tokyo, for furnishing the silicone oil, to Daikin Industries, Ltd., Osaka, and to Asahi Glass Co., Ltd., Tokyo, for kindly furnishing the very pure samples. We also acknowledge Takuhei Shimokawa, Mitsuhiro Yudo, and Takeshi Tamatsu for their valuable cooperation.

Literature Cited

(1) For example, see: Kruse, H. *Int. J. Refrig.* **1981**, *4* (3), 159.
(2) Air Conditioning, Heating & Refrigeration News, July 13, 1987.
(3) Takaishi, Y.; Kagawa, N.; Uematsu, M.; Watanabe, K. *Proc. Symp. Thermophys. Prop., 8th* **1982**, *2*, 387.
(4) Hasegawa, N.; Uematsu, M.; Watanabe, K. *J. Chem. Eng. Data* **1985**, *30*, 32.
(5) Hosotani, S.; Maezawa, Y.; Uematsu, M.; Watanabe, K. *J. Chem. Eng. Data* **1988**, *33*, 20.
(6) Yada, N.; Uematsu, M.; Watanabe, K. *Trans. Jpn. Assoc. Refrig.* **1988**, *5* (1), 107.
(7) Yada, N.; Uematsu, M.; Watanabe, K. *J. Chem. Eng. Data* **1989**, *34*, 431.
(8) Yada, N.; Uematsu, M.; Watanabe, K. *Int. J. Thermophys.* **1989**, *10* (3), 639.
(9) Takaishi, Y.; Uematsu, M.; Watanabe, K. *Proc. Int. Congr. Refrig., 15th* **1978**, *2*, 117.
(10) Takaishi, Y.; Uematsu, M.; Watanabe, K. *Bull. JSME* **1982**, *25* (204), 944.
(11) Tatoh, A. Private communication, 1990.
(12) Valtz, A.; Laugier, S.; Richon, D. *Int. J. Refrig.* **1986**, *9*, 282.

Received for review March 29, 1990. Revised October 23, 1990. Accepted January 10, 1991. We are also indebted to the grant from Tokyo Electric Power Co., Ltd., Tokyo. We are partially indebted to the Grant-in-Aid for Scientific Research Fund in 1989 (Project No. 01603022 and 01790369) from the Ministry of Education, Science and Culture, Japan.

Binary Diffusion Coefficients of the Methanol/Water System in the Temperature Range 30–40 °C

Yeng E. Lee and Sam F. Y. Li*

Department of Chemistry, National University of Singapore, 10 Kent Ridge Crescent, Republic of Singapore 0511

Measurements of the mutual diffusion coefficient of the methanol/water system have been performed by using the Taylor dispersion technique. The results extend over the complete composition range for the mixtures and over the temperature range of 30–40 °C. The system exhibits a minimum in the diffusivity as a function of composition at constant temperature, which is characteristic of alcohol/water mixtures.

Introduction

A knowledge of the transport properties of fluids, i.e. the viscosity, diffusivity, and thermal conductivity, is frequently required for designing new technological processes and also in research work. In particular, diffusion is important in the design of chemical reactors, liquid/liquid extraction units, and absorbers, as well as distillation columns. In addition, the study of fluid-state theory, mass-transfer phenomena, and molecular

0021-9568/91/1736-0240$02.50/0